

"Made available under NASA sponsorship
in the interest of early and wide dis-
semination of Earth Resources Survey
Program information and without liability
for any use made thereof."

KB/mcConnell

E7.3 10780.

CR-133147

Bimonthly Report: 5/4/73 to 7/4/73

ERTS Proposal No. 108

Remote Sensing of Ocean Currents

George A. Maul, Principal Investigator, GSFC ID-CO315

OBJECT

The object of this investigation is to locate ocean current boundaries by sensing the color change associated with the cyclonic edge of the zone of maximum horizontal velocity shear. The test site is the eastern Gulf of Mexico where the strongly baroclinic flow from the Yucatan Straits forms into the Loop Current. The research will attempt to use ERTS data in the investigation of ocean color sensing from simultaneous observations by ship and satellite.

FIELD DATA COLLECTION

A time-series of the Loop Current is being obtained by occupying the suborbital track of ERTS that passes into the Yucatan Straits every 36 days. The research vessel is on the sub-orbital track on the day of satellite transit collecting continuous chlorophyll-a and radiometric temperature (in conjunction with the NOAA-2 IR sensors); hourly (15 km interval) expendable bathythermograph, volume scattering, surface bucket temperature and salinity samples are being obtained. During daylight, spectra of upwelling and downwelling radiance (400-800 nm) are being measured with a $\frac{1}{4}$ meter Ebert scanning spectroradiometer. Upon reaching the Yucatan Straits a temperature/salinity/depth (STD) transect of nine stations is being made in order to determine the geostrophic current and transport fields. After the STD transect, the surface boundary of the Loop Current is being tracked using the same measurements outlined for the sub-satellite track. A second STD transect of the Florida Straits from Key West to Havana is made in order to determine the discharge from the basin.

WORK SUMMARY

One cruise was completed just prior to the start of the reporting period, one cruise was undertaken, and preparations for the July cruise were made. The June cruise marked the first moderate weather all winter; the change was welcomed by all. The

(E73-10780) REMOTE SENSING OF OCEAN
CURRENTS Bimonthly Report, 4 May - 4
Jul. 1973 (National Oceanic and
Atmospheric Administration) 34 p HC

N73-27256

Unclas

CSCL 08C G3/13 00780



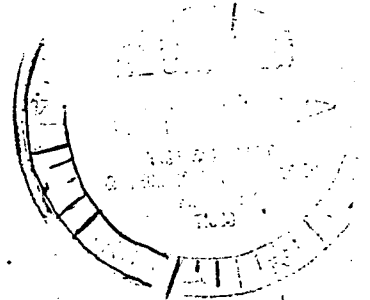
U.S. DEPARTMENT OF COMMERCE
National Technical Information Service
5285 Port Royal Road
Springfield, Virginia 22151

Date: October 4, 1973

Reply to
Attn of: 954.01

Subject: NASA Document Discrepancy Report 73-368

To: Mr. E. E. Baker
Deputy General Manager
Informatics TISCO
P. O. Box 33
College Park, Maryland 20740



Re: N 73-27256

- 1. Page(s) are missing from microfiche and paper copy. Please provide a complete copy. Figures 1 thru 10 indicated by paper clips.
- 2. Portions of this document are illegible when reproduced. Please provide a reproducible copy.
- 3. A microfiche reproduction is not legible. The case file was not received. Please provide at least an acceptable microfiche.
- 4. Incorrectly priced at _____ . It should be _____ for _____ pages. However, price will remain as announced in STAR.
- 5. Case file returned herewith. When correction has been made please return to NTIS or if corrections cannot be made note NASA records that the case file was returned.
- 6. Other:

February 26, 1975

The casefile and microfiche for N73-27256 are forwarded herewith for your retention. These items include figures 1 - 10 noted as missing from our original processing copy.

Sincerely,

E. E. Baker
Deputy General Manager

Phone: 703 -321-8517

FB/BR/djr

PLEASE ATTACH COPY OF THIS LETTER WITH YOUR RESPONSE

cruise is detailed in the attached report.

The PI went to Konstanz, F.R.G. to present an invited paper at the 16th Plenary Meeting of COSPAR entitled, "Applications of ERTS Data to Oceanography and the Marine Environment". Interest was expressed in the USA's work in this field by several countries; all 200 preprints were taken by attenders. A copy, less the photographic figures, is attached.

The PI, Mr. R. L. Charnell, and LTJG R. M. Qualset went to the Image Processing Laboratory at JPL under MESA (NOAA) funds on 25-29 June 1973. IPL's group under Mr. F. C. Billingsley ran a series of test runs on the 16 August New York Bight scene to determine what routines of their VICAR system would be useful in analyzing ERTS data for the ocean scene. The results of various successful contrast stretching attempts on NOAA equipment has been reported on earlier. Several display techniques using false color were investigated for ratios, summations, and summation ratios. The effects of several smoothing routines on the data were studied along with their effect on mathematically generated discrete fields. Many of the image output results are not available at this writing and certainly little digestion has taken place. Several techniques show promise and several showed that not only can false interpretations be enhanced but false data can be manufactured when working with the low radiances in the ocean scene. One result of this investigation has been to request NASA to turn on the high gain mode of the MSS over the ocean for at least one test. The preliminary results of the IPL work will be presented at the Annual Meeting of the American Society of Photogrammetry in October 1973.

WORK PLANS

If the Loop Current separates into a detached anticyclonic eddy by this cruise, the August cruise will be the last in the time-series by ship and satellite. It is then our plans to stop requesting ERTS data over the whole area and just look at a few key points for the lifetime of the satellite. The New York Bight, the SE coast of Florida, and one suborbital track into the Gulf of Mexico are all that will be needed.

Much of the upcoming bimonthly period will be taken up by leave, routine data processing, and cruises. Hopefully, with the end of the field experiment, more time will be available to study the spectral data and its application to the MSS sensors.

George A. Maul
 July 6, 1973
 NOAA/AOML-PhOL
 15 Rickenbacker Causeway
 Miami, Florida 33149

3

NATIONAL OCEANIC AND ATMOSPHERIC ADMINISTRATION
ATLANTIC OCEANOGRAPHIC AND METEOROLOGICAL LABORATORIES
PHYSICAL OCEANOGRAPHY LABORATORY
NASA/GSFC

CRUISE REPORT
R/V VIRGINIA KEY

1-7 June 1973

I. OBJECTIVES

The purpose of this cruise was to continue a time series of the location of the Loop Current as part of AOML's project with the Earth Resources Technology Satellite (ERTS) and the NOAA-2 Meteorological Satellite. The research is intended to obtain baseline information on the spectroradiometric properties of the ocean's surface useful for remote sensing and the detection of that information at orbital altitudes.

II. SCHEDULE

<u>Date</u>	<u>Time</u>	<u>Activity</u>
June	DST	
1	0600	Depart Miami
2	0130	Commenced STD transect of Florida Straits
3	1100	Commence STD transect of Yucatan Straits
4	0600	Commence tracking current
	1000	Satellite Transit
6	1800	Complete survey
7	1000	Arrive Key West

III. STATION POSITIONS

The northern limit STD transect of the Florida Straits was at the 100-fathom curve south of Marquesa Key Light and

terminated 12 n. mi. north of Havana Cuba. The station locations were:

24°21'N	82-09W	Station 1
24°11'N	82-16W	2
24°05'N	82-18W	3
23°55'N	82-23W	4
23°46'N	82-27W	5
23°36'N	82-29W	6
23°21'N	82-28W	7

The station locations for the Yucatan Straits STD transect were:

21°50'N	85-11'W	Station 8
21°48'N	85-21'W	9
21°43'N	85-32'W	10
21°42'N	85-42'W	11
21°40'N	86-06'W	12
21°36'N	86-13'W	13
21°36'N	86-22'W	14
21°31'N	86-32'W	15

The easternmost station was 12 n. mi. west of Cabo San Antonio; the westernmost station was 12 n. mi. east of Isla Contoy.

The cruise from Isla Contoy to Dry Tortugas was a saw-toothed path, which crossed the surface boundary layer zone of the current.

IV. PERSONNEL

George A. Maul, Chief Scientist	NOAA/AOML
Michael Ednoff	FSU
Johnny Holmes	University of Miami
Gary Waldo	USF

V. DESCRIPTION OF OPERATIONS

Data collection commenced with an STD transect of the Florida Straits. Continuous flow measurements of chlorophyll-a and continuous radiometric sea surface temperature were recorded on a dual channel recorder. While on the track, hourly XBTs, surface bucket temperature, surface salinity, and measurements of scattering ratios were taken. Spectra of upwelling and downwelling visible radiation were not observed. Loran A fixes were made at one hour

intervals and at major course, and/or speed changes. One liter samples were filtered for a spectrophotometer calibration of chlorophyll-a every six hours and at major changes in the fluorescence, and for biological samples.

Good weather plus cooperation from Maurice Rinkel aboard the R/V BELLOWS, made tracking the large extent of the Loop Current possible as the current continued to grow in the Gulf of Mexico. A project to find sargassum in and out of the Loop Current was not very successful due to lack of encountering any heavy patches of sargassum. Radio communications on 2182 KH₂ with R/V BELLOWS was poor due to the low output of the R/V VIRGINIA KEY's set; it is recommended that crystals for 2182, 2670, and 2638 KH₂ be obtained.

VI. LOGS

- Chief Scientist Log
- Deck Log
- Track Chart
- Loran Log (C&GS 722)
- Hydrographic Station Log
- Bathythermograph Log

Submitted by: George A. Maul
June 10, 1973

6

APPLICATIONS OF ERTS DATA TO OCEANOGRAPHY
AND THE MARINE ENVIRONMENT

George A. Maul

National Oceanic and Atmospheric Administration
Atlantic Oceanographic and Meteorological Laboratories
Miami, Florida 33149, U.S. A.

The multispectral scanner (MSS) on board the Earth Resources Technology Satellite (ERTS) has returned some remarkable imagery with applications to oceanography. Theoretical background for understanding the penetration and reflectance of light from the sea is briefly given for the MSS bands. Examples from the recent symposium on significant results include studies of sea ice, fisheries, charting, beach erosion, limnology, estuarine circulation, ocean features in the lee of islands, ocean currents, and internal waves. Several enhancement techniques are discussed and exemplified in the context of its application.

INTRODUCTION

The attenuation coefficient (α) for light traveling through water is dependent on its wavelength (λ). The attenuation coefficient is defined as the sum of the absorption coefficient (a) and the scattering coefficient (b). A general minimum occurs near 0.5 μm with several orders of magnitude increase near 1.1 μm . These wavelengths represent the lower cutoff of MSS-4 (0.5-0.6 μm) and upper cutoff of MSS-7 (0.8-1.1 μm) of the multispectral scanner (MSS); MSS-5 (0.6-0.7 μm) and MSS-6 (0.7-0.8 μm) are intermediately situated. The underwater irradiance (H) in each of these bands is given by

$$H(\phi, z) = \int_0^{\infty} \phi(\lambda) H_0(\lambda) \exp. \left[- \int_0^z \alpha(z, \lambda) dz \right] d\lambda$$

where ϕ is the response of the bandpass filter, H_0 is the irradiance at the sea surface, and z is depth.

Calculations for the ERTS bands, normalized, and expressed in percent, are graphically depicted in figure 1[1]. Of the energy that penetrates pure water, MSS-7 has an inverse e-folding depth of much less than 1 meter, whereas MSS-4 decays to 1/e of its surface value at approximately 20 meters. These are optimistic by a factor of at least 2, for even the cleanest seawater has α values double that of pure water. Practically, water information

in MSS-6 and 7 are constrained to be surface features, whereas MSS-4 and 5 can offer information at depth.

Chandraeskar^[2] formulated an expression for the reflectance $R(z, -)$ at the sea surface from the theory of radiative transfer. Reflectance is defined as the ratio of the upwelling (-) to the downwelling (+) irradiance. At the sea surface, $z = 0$, and for the simple case of isotropic scattering,

$$R(z, -) = 1 - H(\mu, \omega_0) \sqrt{1 - \omega_0}$$

where ω_0 , the scattering albedo, is the ratio of the scattering coefficient to the attenuation coefficient, $H(\mu, \omega_0)$ are the H-functions tabulated by Chandraeskar, and μ is the cosine of the zenith angle. The significant variable is ω_0 . Examining the two limiting cases, note that R approaches 1 when ω_0 approaches 1 (scattering dominant) and as ω_0 approaches 0 (absorption dominant), R approaches 0 because $H(\mu, 0) = 1$. Thus if all the light that enters the ocean is scattered, reflectance is 100% and the ocean appears white, and if all the light is absorbed, reflectance is zero and the ocean is black.

The upwelling irradiance above the sea surface is the sum of $R(z, -)$ plus the reflection from the surface of direct and diffuse sunlight. Three spectra taken with near equal

solar zenith angles, differing chlorophyll-a concentration (affecting absorption, a) and differing volume scattering coefficients $\beta_{4,5}$ (affecting scattering, b) are given in Fig. 2. These are irradiance measurements taken from ship-board at 4 meters above the surface in the Straits of Florida; water depth was in excess of 100 meters. These measurements are in qualitative agreement with calculations made from isotropic reflectance theory given above, and serve to give relative energy levels for MSS-4, 5, and 6 for different oceanic waters. Clearly ERTS bands have information in them on the biomass of the ocean.

The radiant intensity $N(\lambda, \theta)$ from a nadir angle θ received at the satellite is attenuated by absorption and scattering in the atmosphere. For Rayleigh scattering, Beer's Law gives an exponential solution with a scattering coefficient

$$S(\lambda) = \frac{32 \pi^3 (n(\lambda) - 1)^2 \rho}{3 \lambda^4 N \rho_0}$$

where N is the number of molecules at STP, n is the index of refraction at STP, ρ_0 and ρ are the standard and actual densities of dry air. This brings out the well-known inverse fourth power law. Integration over the spectral response of the MSS filters would give approximate scattering ratios of 9:5:3:1 for the MSS-4, 5, 6, and 7 respectively. For the same

surface signal, contrast is reduced by a factor of almost 2 when viewing in MSS-4 as compared to 5. Many authors report most satisfactory oceanographic results using MSS-5 for this reason.

SIGNIFICANT RESULTS

In the sections that follow the work of several contributors to the Symposium on Significant Results Obtained from ERTS-1 are summarized. The figures were given by the authors as representative of their work. Where results are not specifically from the symposium, the proper reference is given at the conclusion of the paper.

SEA ICE

Barnes reports that sea ice is detectable in all of the MSS bands and can be distinguished from clouds through a number of interpretive keys. Overall, MSS-4 and 5 appear to be better for mapping the ice edge, whereas MSS-7 provides greater detail in the ice features. Fig. 3 is imagery showing sea ice along the east coast of Greenland on 25 September 1972. The left-hand image is MSS-4 and the right-hand image is MSS-7. Differences in the reflectance in the two spectral bands are believed to be associated with different ice types. Areas of probable brash or rotten ice have a considerably higher

reflectance in MSS-4 than in MSS-7; however, ice floes that are difficult to distinguish in MSS-4 have a significantly higher reflectance than the surrounding brash ice in MSS-7. Many surface features on ice floes can be seen in MSS-7; this is caused by the high absorption of liquid water in the near infrared (MSS-7).

FISHERIES

Kemmerer and Benigno studied the application of spacecraft data to the Menhaden fisheries in the Mississippi Sound region of the northern Gulf of Mexico. The goal here is to improve fisheries by locating areas of potentially high yield. MSS-5 proved to be most useful in these efforts. Multiple regression analysis of oceanographic variables collected during satellite transit showed that water depth and turbidity had statistical significance with fish catch data; this is confirmed by Maughan, Marmelstein, and Temple. Fig. 4 is a false color density slice of MSS-5, taken on 5 August 1972. In this technique a color is assigned to each of several discrete photographic densities (gray shades). The black dots are areas of fish school locations observed during transit. Each color represents a narrow density range within the range containing the fish school locations; the fish

schools fall either adjacent to or within this narrow range. Szekiolda and Curran report correlation with ocean chlorophyll measurements of the ratio MSS-4/MSS-5; the higher the ratio the more chlorophyll. This is in part supported by the data of fig. 2 if ω_0 behaves in a consistent manner.

CHARTING

Shoreline information needed to update nautical charts and maps is emphasized on MSS-7, whereas shallow bathymetric features are available in MSS-4 and 5. Fig. 5 is from Williams and shows images in MSS-4, 5, and 7 and a conventional map of the Cape Cod area on 1 September 1972. There are many inaccuracies in the portrayal of the coastline and inland lakes when compared with the imagery. The discrepancies are caused by cartographic generalization from larger scale maps and, in some instances, actual changes in landforms. The imagery provides a very cost-effective method for increasing map accuracy, portraying additional environmental information, and for frequent updating at scales of 1:250,000 or smaller. Polcyn has obtained correlations over the Bahamas banks of depth measurements at 2, 3, and 8 meters; a mathematical model for depth measurements using ratios of MSS-4 and 5 has been developed. Ross found that where reflective bottom and

clear water are found, MSS-4 images can be used with density contouring for estimating depths in 2, 5, and 10 meter steps. These findings may provide significant data for assisting in the verification of navigation hazards in remote areas as well as updating other chart products.

BEACH EROSION

Slaughter has been applying ERTS aircraft photographs to determine the relationship of existing groins. This is being done to determine if further groin construction is warranted. Kerhin has been using similar imagery for recognition of beach ridges and sand waves. The ERTS imagery has marginally useful resolution for the features themselves; however, indirect information, such as sediment transport patterns inferred from the imagery (see below) will prove useful in this regard.

LIMNOLOGY

Strong made an observation of an algae bloom on Utah Lake on 12 September 1972. Fig. 6 shows an anticyclonic gyre in this shallow (ca. 3m) and highly eutrophic lake. The imagery is an example of color infrared image reconstruction. MSS-4, 5, and 6 were registered and projected on the same screen through blue, green, and red filters respectively. The algae are highly reflective in MSS-6 and appear red on the color

composite. Utah Lake is known for its high turbidity, and during summer months algae blooms frequently follow calm periods. Brigham Young University conducted a limnology survey on the day of satellite transit and found an extensive algae cover, mostly Anabeana, that was several centimeters thick.

ESTUARINE CIRCULATION

Certain estuaries, such as Cook Inlet in Alaska, are so large that conventional survey techniques may lead to erroneous conclusions concerning the overall circulation patterns. Wright, Sharma, and Burbank used natural tracers such as the fine sediment (glacial flour) from deglaciation to study water movements. MSS-4 and 5 were the best bands for these waters where suspended sediment loads range over 400 mg/l. The ERTS imagery was useful in identifying the boundary between fluvial waters and marine waters. This boundary is important because almost all pollutants are associated with turbid waters; further, location is valuable to commercial fisheries because fish congregate there and for navigation safety because logs and other flotsam accumulate at such boundaries. Several new features of the water movements have been identified from ERTS imagery with surface vessel support. Another example of application to estuaries is given in fig.

7 from Klemas, Srna, and Treasure. Two views of Delaware Bay are given in this figure at different stages of the tidal cycle. The images are MSS-5 showing the clear (darker) near-shore water entering the bay; ebbing waters have high turbidity. The patterns are in general agreement with the tidal current charts for the time of transit. Thus, in this shallow estuary natural traces can be used for environmental studies just as in the deep regime of the fjord-like Cook Inlet.

OCEAN CURRENTS

Detection of baroclinic flows in the subtropics is not possible on a year-round basis by infrared techniques because the sea surface becomes seasonally isothermal in many areas. The location of water masses in hurricane-prone areas such as the Gulf of Mexico is important to transportation, fisheries, and weather forecasting. Maul is making cruises every 36 days into the Gulf to locate the Loop Current by ship and satellite. The findings to date have been several-fold: The edge of the current is an accumulation zone for surface algae and phytoplankton which frequently delineate the boundary by high reflectance in MSS-6. In addition a change of sea state frequently occurs; steeper waves and more whitecaps occurring in the current. Fig. 8 shows how the cyclonic edge of the current has been detected by ERTS

supported by concurrent surface observations. The left-hand panel (MSS-4) shows the greener (lighter shade) water of Florida Bay delineating the edge of the bluer (darker shade) Loop Current. This is an expected consequence of analysis of the data in fig. 2. The right-hand panel (MSS-5) shows the current appearing brighter than the surrounding waters. Maul interprets this as the overriding influence of whitecaps and foam in the higher sea state of the current and suggests that a sea state correction measurement is necessary in order to quantify any ocean color measurements. Alternately, the possibility exists that the MSS observations could be used to estimate sea state.

OCEAN FEATURES IN ISLAND LEES

Hanson, Hebard, and Cram are studying the application of ERTS data to locating eddies in the lee of the Antilles. These eddies are known zones of high productivity and possibly good tuna fisheries. Fig. 9 is a mosaic of images from two consecutive days. These are negative prints so that the lighter appearing features to the west of the islands are regions of low reflectance. Note also the rapid change in these features, particularly in the lee of St. Vincent where the one-day delay in adjacent transits produces a remarkable change in the imagery. Hanson^[3] has shown that these features aline with the local wind and may be caused by a modification

of the sea and/or swell in a wind shadow of the island. The features are seen in all bands and hence are surface phenomena but have not been confirmed in ground truth cruises to date. A firm conclusion as to the cause of these features has not been reached nor has the impact of their existence on the environment been analyzed.

INTERNAL WAVES

Apel^[4] has interpreted the wavelike features of fig. 10 as surface manifestations of internal waves. The patterns on this image are in agreement with refraction patterns computed for internal waves of 1000-meter wavelength for the bathymetry in the southeastern New York Bight. The left-hand panel is a contrast stretched computer enhancement of the original scene (right-hand panel) by Maul, Charnell, and Qualset^[5]. The contrast stretching technique is to assign all values above a certain cutoff on the MSS digital tapes to the highest exposure and all those below another threshold to the lowest exposure. Thus, only the radiance steps of interest are assigned the intermediate gray levels, and many significant portions of the ocean scene are revealed. In this case the surface reflection patterns generated by the slick water/rough water patterns, typical of these waves, are markedly enhanced.

CONCLUSIONS

ERTS has proven itself to be a valuable tool to oceanographers in many disciplines. In several cases it has provided the first repetitive synoptic view with high spatial resolution ever obtained. Observations have been made of the effect man has on his environment^[1], and in this way the data have focused attention on new or emerging problems. The problem of scientifically correlating these data with additional surface measurements and optimizing multispectral pattern recognition lies ahead. Indeed the labor and the reward of ERTS are just beginning to surface.

REPRODUCIBILITY OF THE ORIGINAL PAGE IS POOR

REFERENCES

1. R.L. Charnell and G.A. Maul Nature, 242, 451-452, 1973.
2. S. Chandrasekhar Radiative Transfer, Oxford University Press, London, 393pp, 1950.
3. K.J. Hanson, N.O.A.A./A.O.M.L., personal communication, 1973.
4. J.R. Apel, N.O.A.A./A.O.M.L., personal communication, 1973.
5. G.A. Maul, R.L. Charnell, and R.H. Qualset October 1973 Meeting of the American Society of Photogrammetry (in preparation), 1973.

Figure 1. Percent of the light that penetrates a column of pure water reaching a given depth for the four MSS bands (after Charnell and Maul[1]).

Figure 2. Spectra of upwelling irradiance taken from 4 meters above the sea surface in the Straits of Florida during 1-4 November 1972. The solar zenith angle was about 30° ; sea state, wind speed, percent cloudiness, and downwelling skylight were approximately the same. The volume scattering function β_{45} is for blue ($0.436\mu\text{m}$) light.

Figure 3. Sea ice detected in MSS-4 (left) and MSS-7 (right). The larger floes in the image are 20-30 kilometers across (after Barnes).

Figure 4. Location of Menhaden schools in the Mississippi Sound are shown by black dots. The false color density slice of MSS-5 shows that the fish locations are just in, or adjacent to, regions of high turbidity (orange). Horizontal scale is approximately 50 kilometers (after Kemmerer and Benigno).

Figure 5. MSS-4 (upper left), MSS-5 (upper right), MSS-7 (lower left) and a conventional map of the Cape Cod area. Horizontal scale on the images is approximately 80 kilometers (after Williams, EROS Program, USGS).

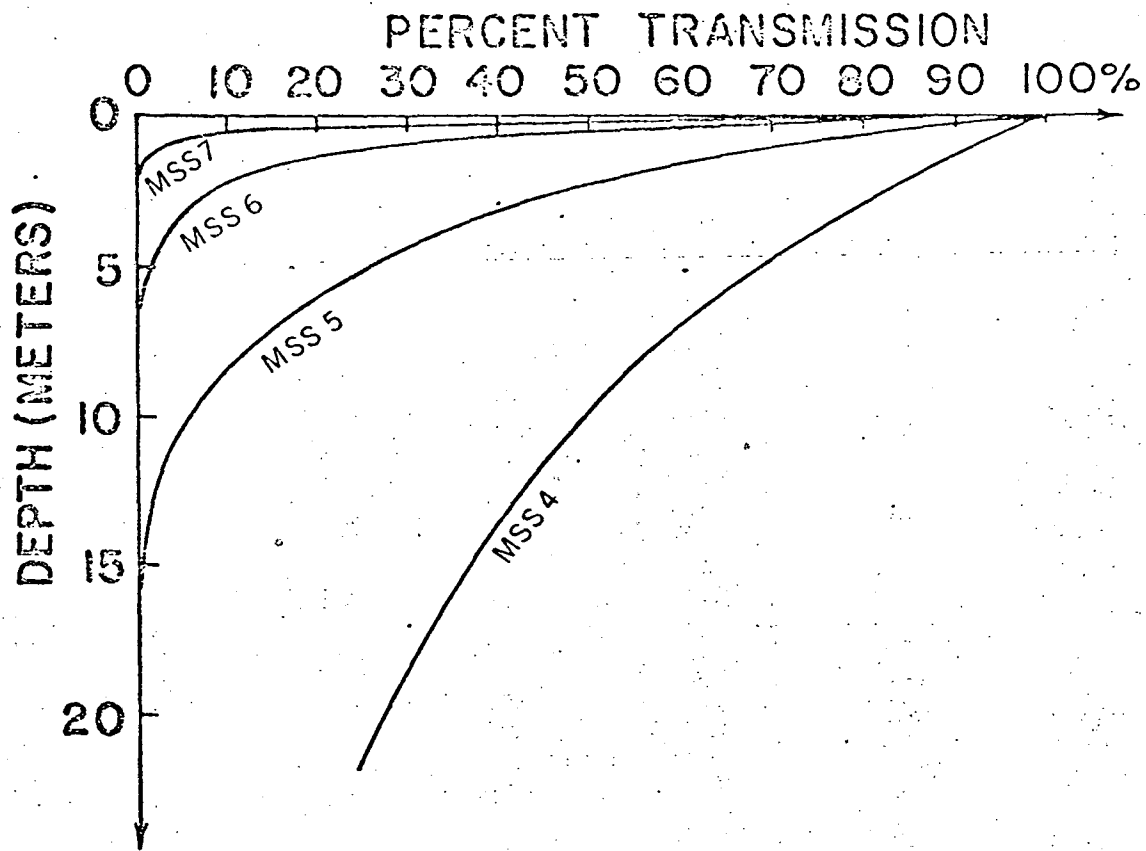
Figure 6. Color infrared recomposition of MSS-4 (blue), MSS-5 (green), and MSS-6 (red) over Utah Lake. The area of the lake is about 375 square kilometers (after Strong).

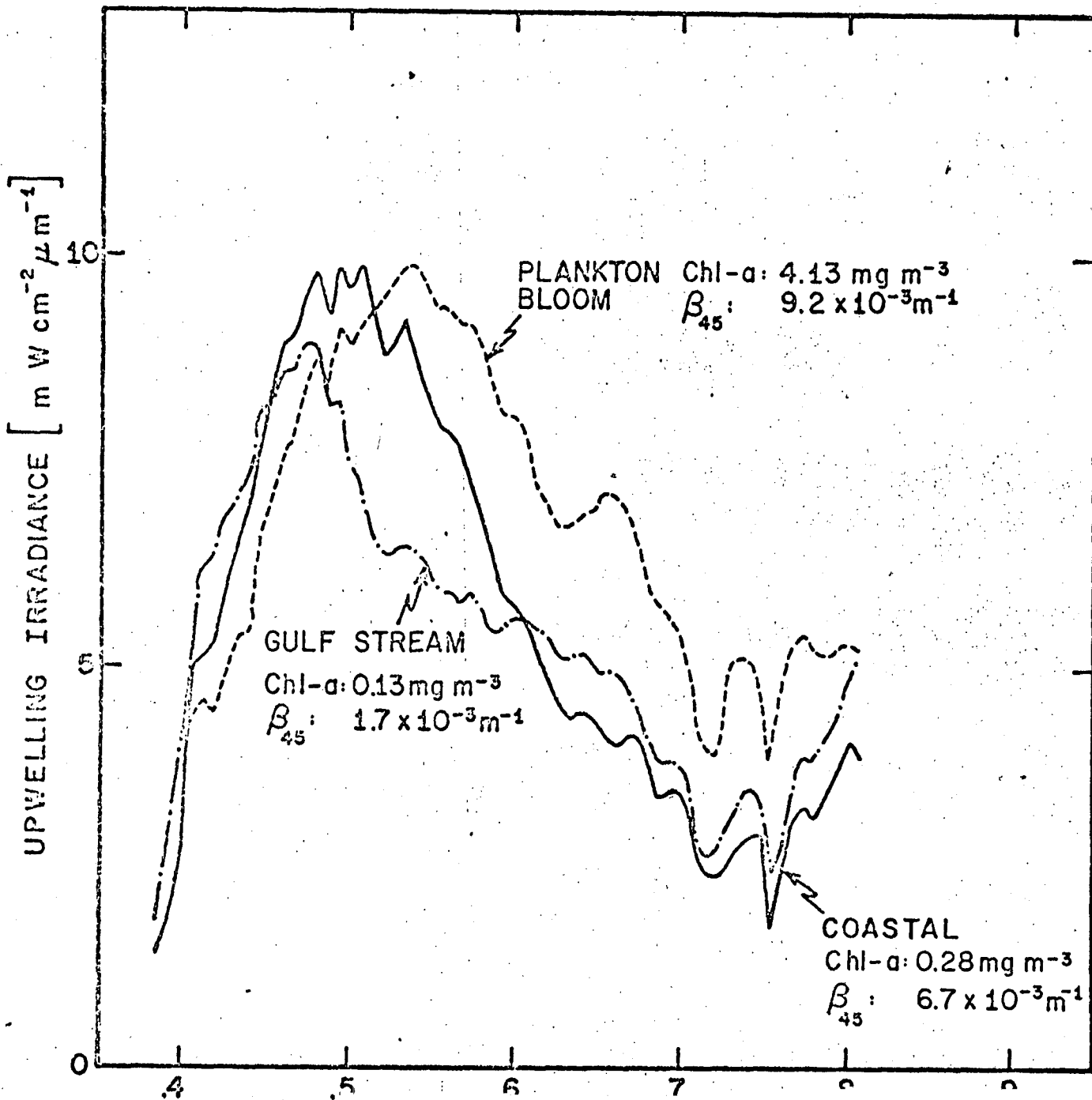
Figure 7. Two views of Delaware Bay at different stages of the tidal current cycle; two hours before maximum flood at the bay entrance (upper) and two hours after maximum flood (lower). These are compared with conventional National Ocean Survey (NOAA) tidal current charts (after Klemas, Srna, and Treasure).

Figure 8. The cyclonic boundary of the Loop Current in the Gulf of Mexico seen in MSS-4 as a consequence of the color change between the coastal water and the current (left), and as a result of higher sea state and hence higher reflectance (right) as seen in MSS-5. Horizontal scale is 180 kilometers in each scene (after Maul).

Figure 9. Low reflectance features in the lee of the Antilles appear brighter on this negative print mosaic. Sketch to the right outlines the features in an area of known eddies (after Hanson).

Figure 10. Contrast stretched computer enhancement (left) of patterns interpreted by Apel[4] to be surface manifestations of internal waves impinging on the continental shelf off New York. Horizontal scale in the enhancement by Maul, Charnell, and Qualset[5] is about 60 kilometers.





REPRODUCIBILITY OF THE ORIGINAL PAGE IS POOR

REPRODUCIBILITY OF THE ORIGINAL PAGE IS POOR

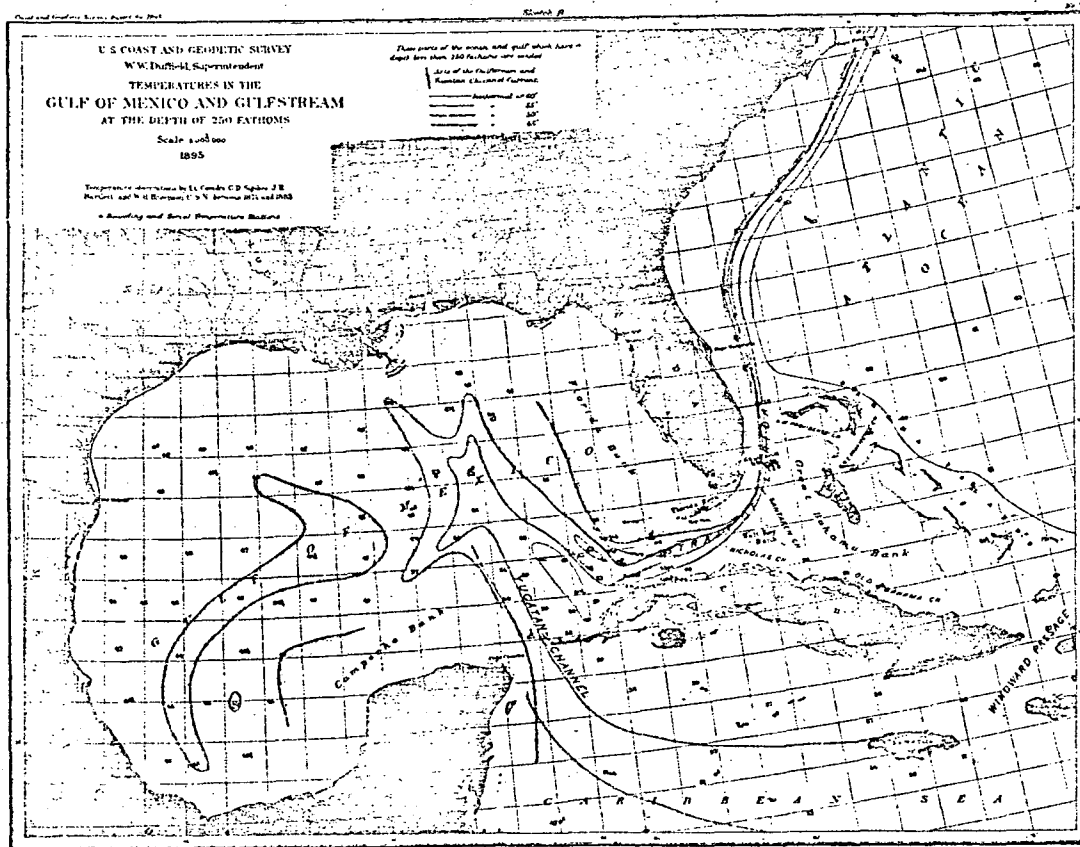


Figure 1. Lindenkohl's 1895 map of the temperature field (°F) at 250 fathoms in the Gulf of Mexico. Data are from soundings made by Sigsbee, Bartlett, and Brownson between 1874 and 1883. The shallow waters (<250 fms) of Campeche Bank and the west Florida Shelf, stippled on the chart, outline the topographic constraints of the Gulf Loop Current.

REPRODUCIBILITY OF THIS ORIGINAL PAGE IS POOR

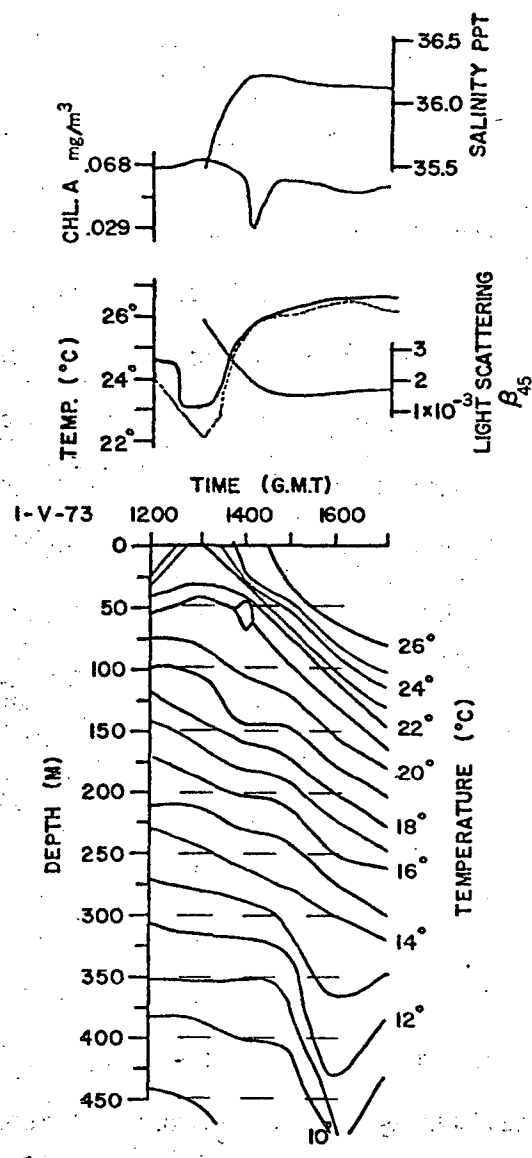


Figure 2. Thermal cross-section of the Gulf Loop Current on 1 May 1973 northwest of Dry Tortugas. Horizontal distance for the five-hour run is 90 kilometers. Bucket temperature (hourly) is solid line and radiometric (10.5 - 12.5 μm) temperature is dashed; other variables connect to their respective ordinate. The indicator isotherm is 22°C at 100 meters, which is approximately 20 kilometers to the right of the maximum surface thermal gradient facing downstream.

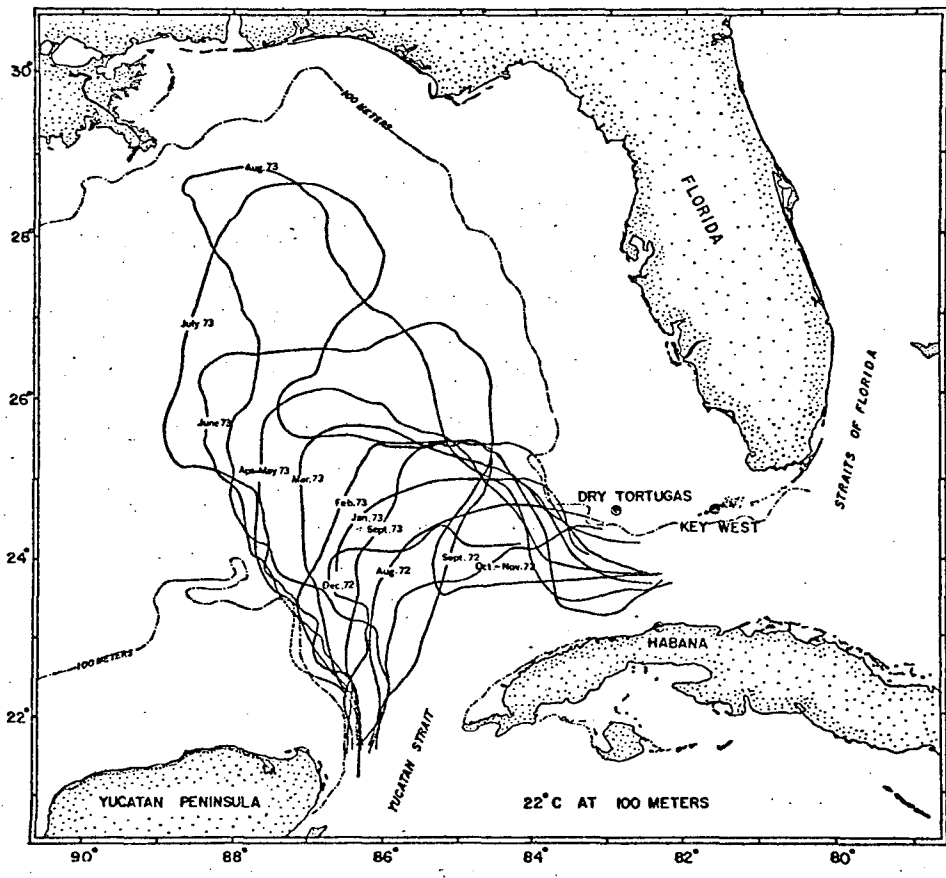


Figure 3. Pathlines of the 22°C isotherm at 100 meters from August 1972, through September 1973. Surveys were 36 days apart and in coincidence with every other transit of the Earth Resources Technology Satellite: where two months are given, the survey extended over the change of date. Cruises were from three to six days in duration and the research ship motored with a following current.

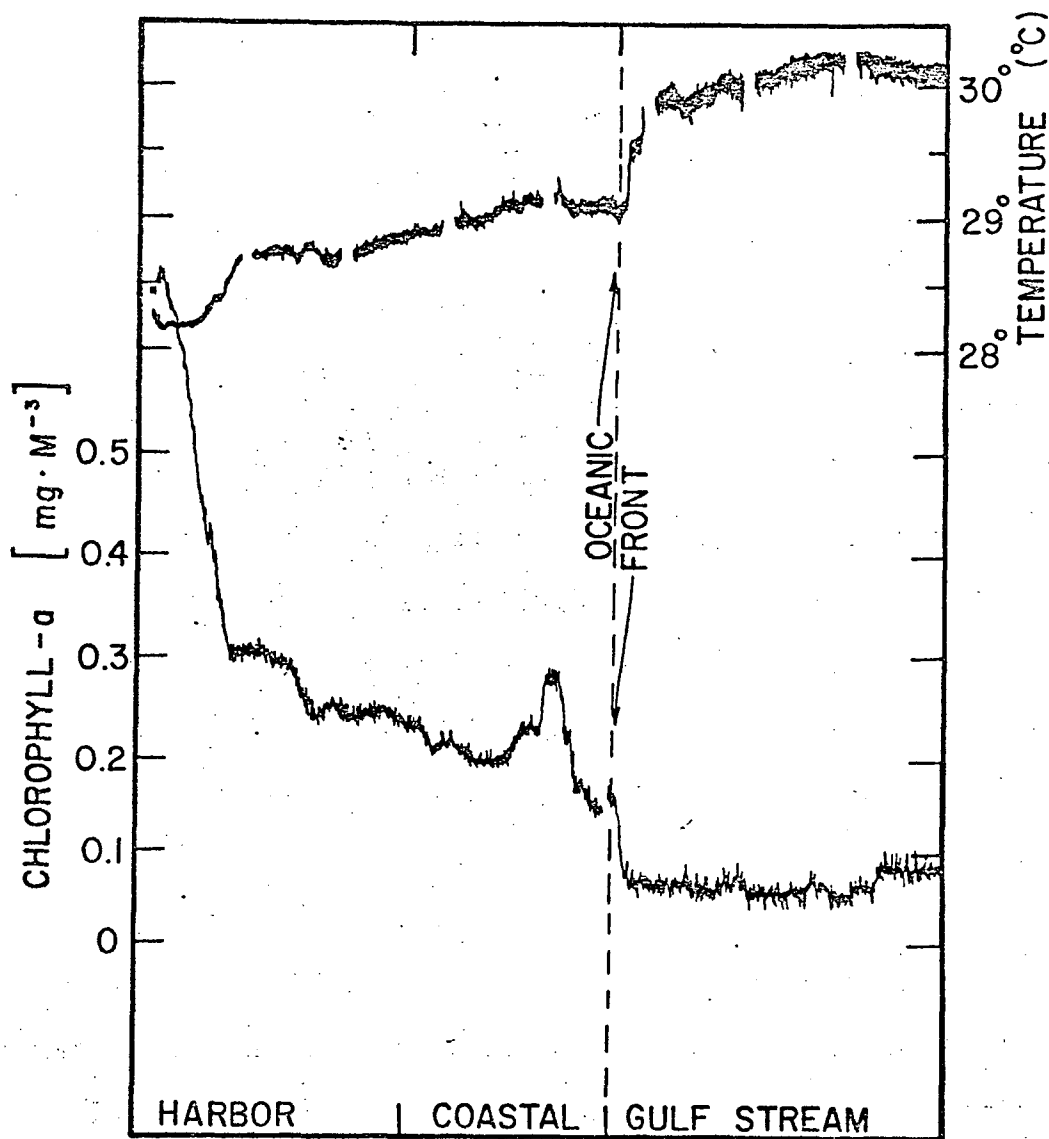


Figure 4. Surface temperature trace (upper) and surface chlorophyll-a profile (lower) across the Loop Current Front and into Key West Harbor. Horizontal scale across the figure is approximately 75 kilometers.

REPRODUCIBILITY OF THE
ORIGINAL PAGE IS POOR

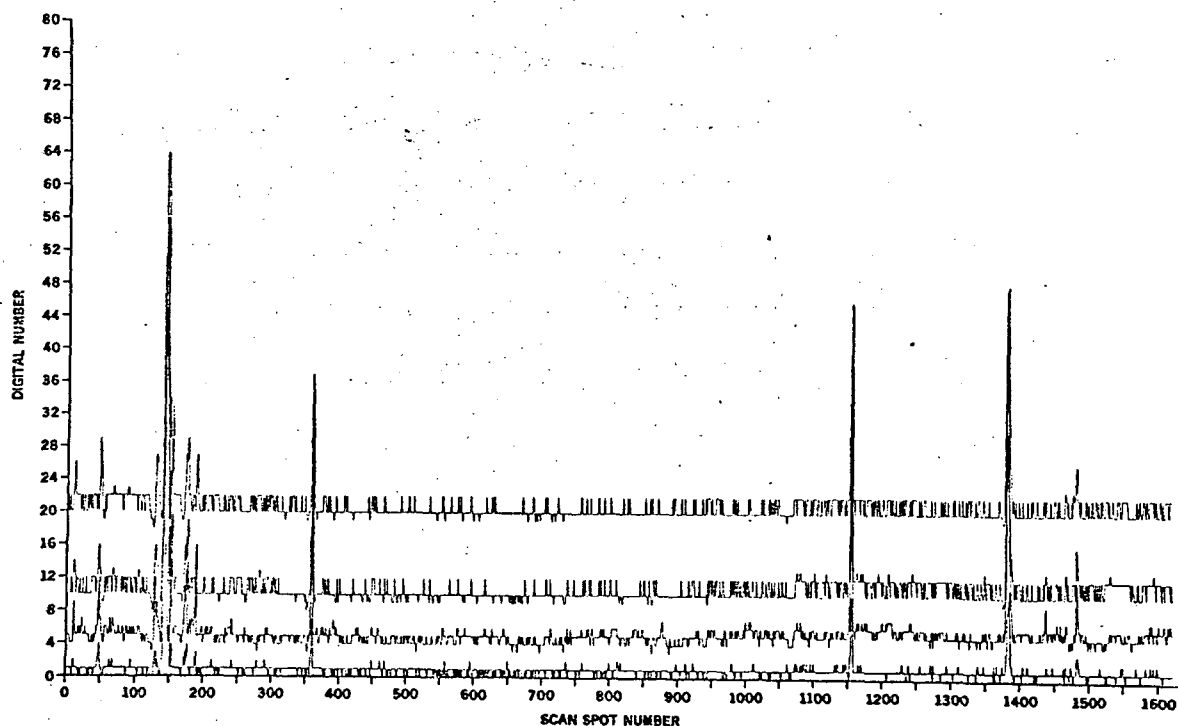


Figure 5. ERTS scanline plot across the Loop Current front. Top scanline is MSS 4, next MSS 5, MSS 6 and MSS 7 on the bottom. The large energy spikes are clouds. At scan spot number 950 there is an increase in the average value of the digital number of 1 or 2; this marks the cyclonic edge of the current.

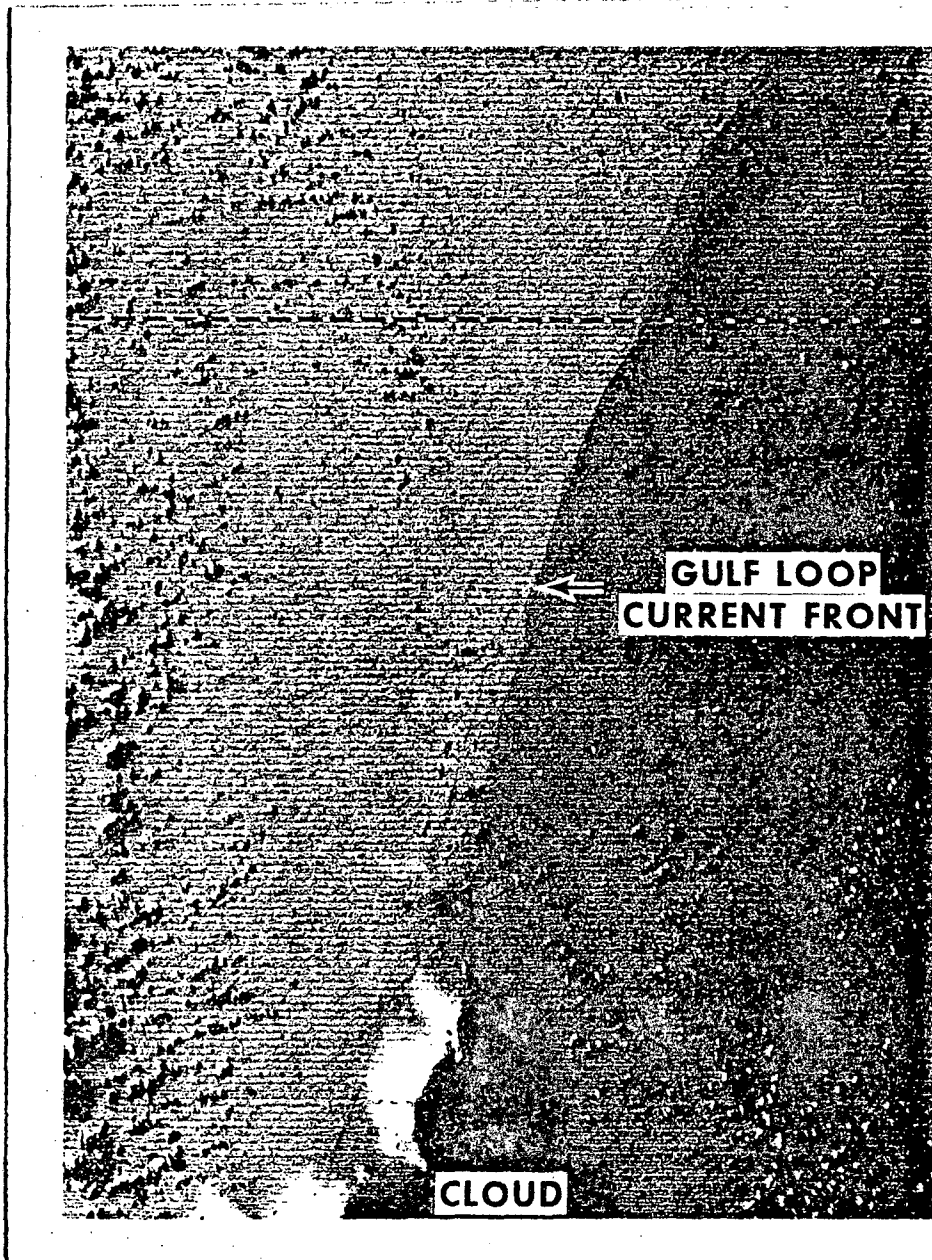


Figure 6. Negative print of computer enhanced ($9 < DN < 13$; $n = 1$) MSS 5 image of the cyclonic boundary of the Gulf Loop Current. Surface vessel track confirmed the location of the current to be the darker shade (higher radiance) region on the right hand side of the image (ERTS ID 1065-15411). Scanline plot in figure 5 horizontally passes through the middle of the scene. Horizontal distance across the image is 90 kilometers.

REPRODUCIBILITY OF THE
ORIGINAL PAGE IS POOR

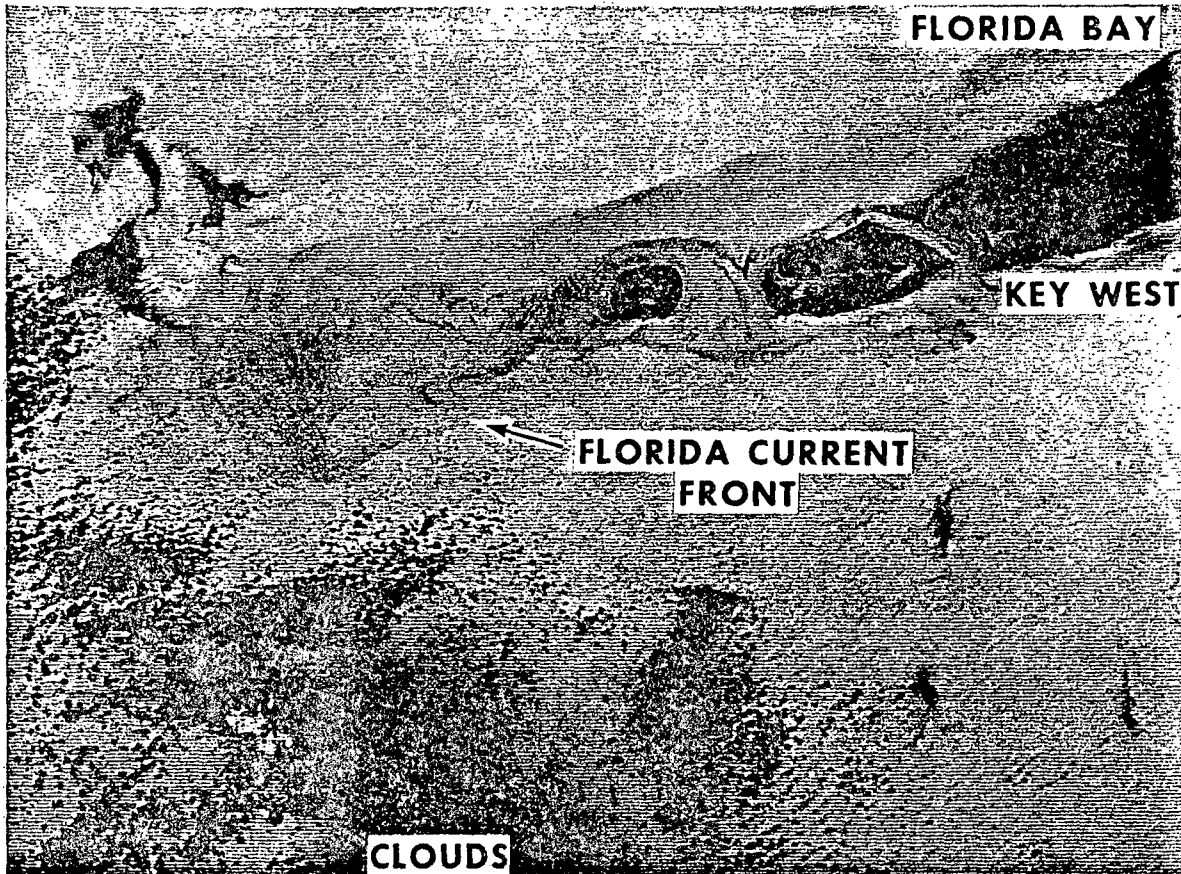


Figure 7. Negative print of computer enhanced ($7 < DN < 15$; $n = 2$) MSS 5 image of Marquesa Key and Key West (ERTS ID T099-15293). Change in radiance southwest of Marquesa from dark to light marks the ship located boundary between the higher intensity Florida Bay water and the lower intensity Gulf Stream. Bottom depth is in excess of 100 meters and thus does not contribute to the radiance. Horizontal distance across the image is 135 kilometers.

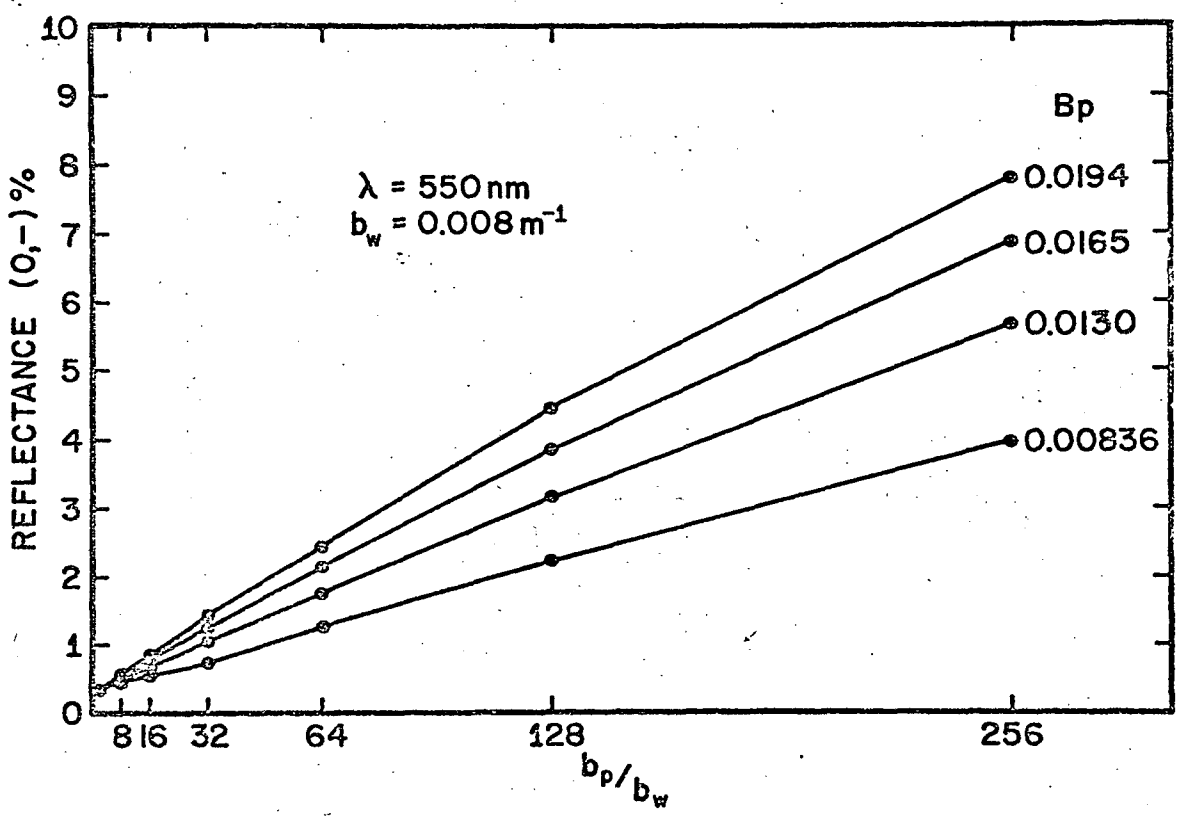


Figure 8. Computed reflectance in percent at the sea surface as a function of the ratio of the particle scattering coefficient to the water (only) scattering coefficient for 550 nm. The value of the fraction of backscattered light due to particles (B_p) for each curve is given on the right hand side.

REPRODUCIBILITY OF THE
ORIGINAL PAGE IS POOR

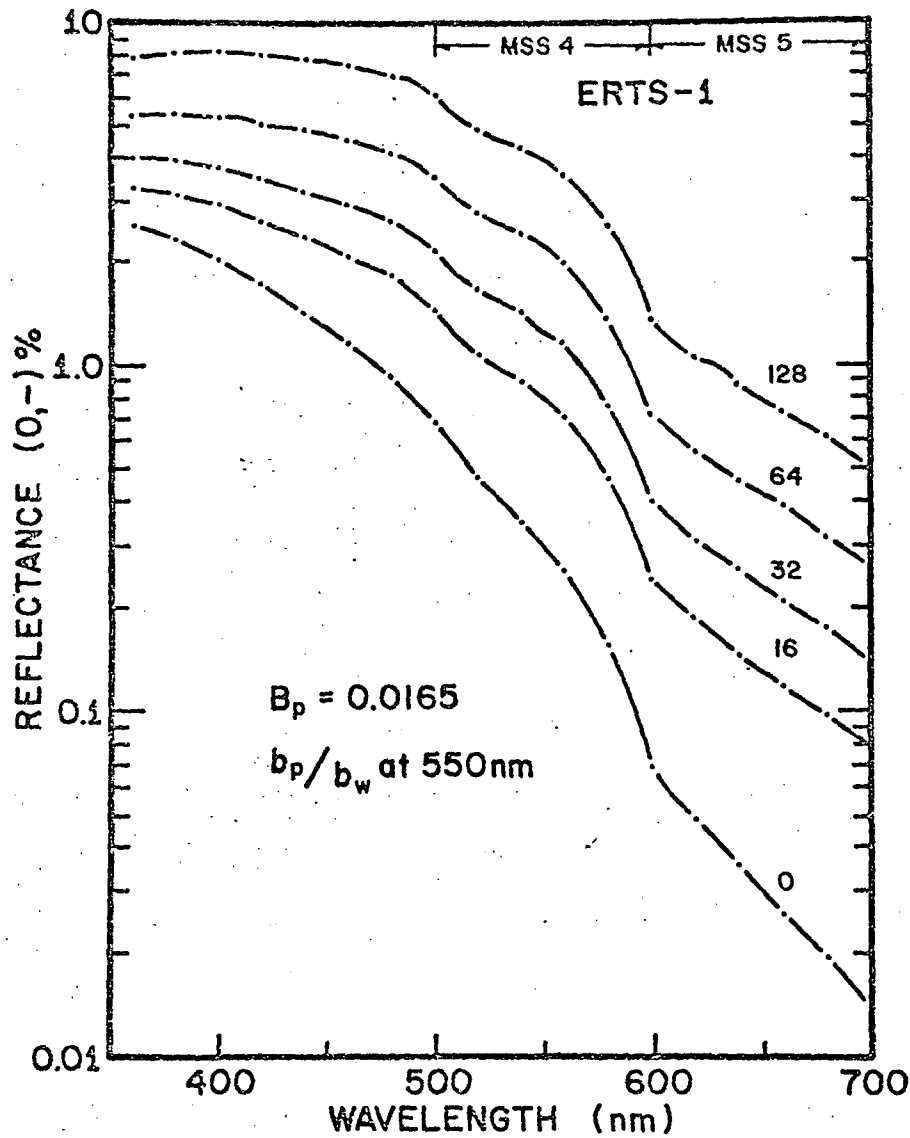


Figure 9. Computed reflectance in percent at the sea surface as a function of wavelength for various values of the ratio of the particle scattering coefficient to the water scattering coefficient. Note the wavelength dependence in these spectra of changing the particle concentration only.

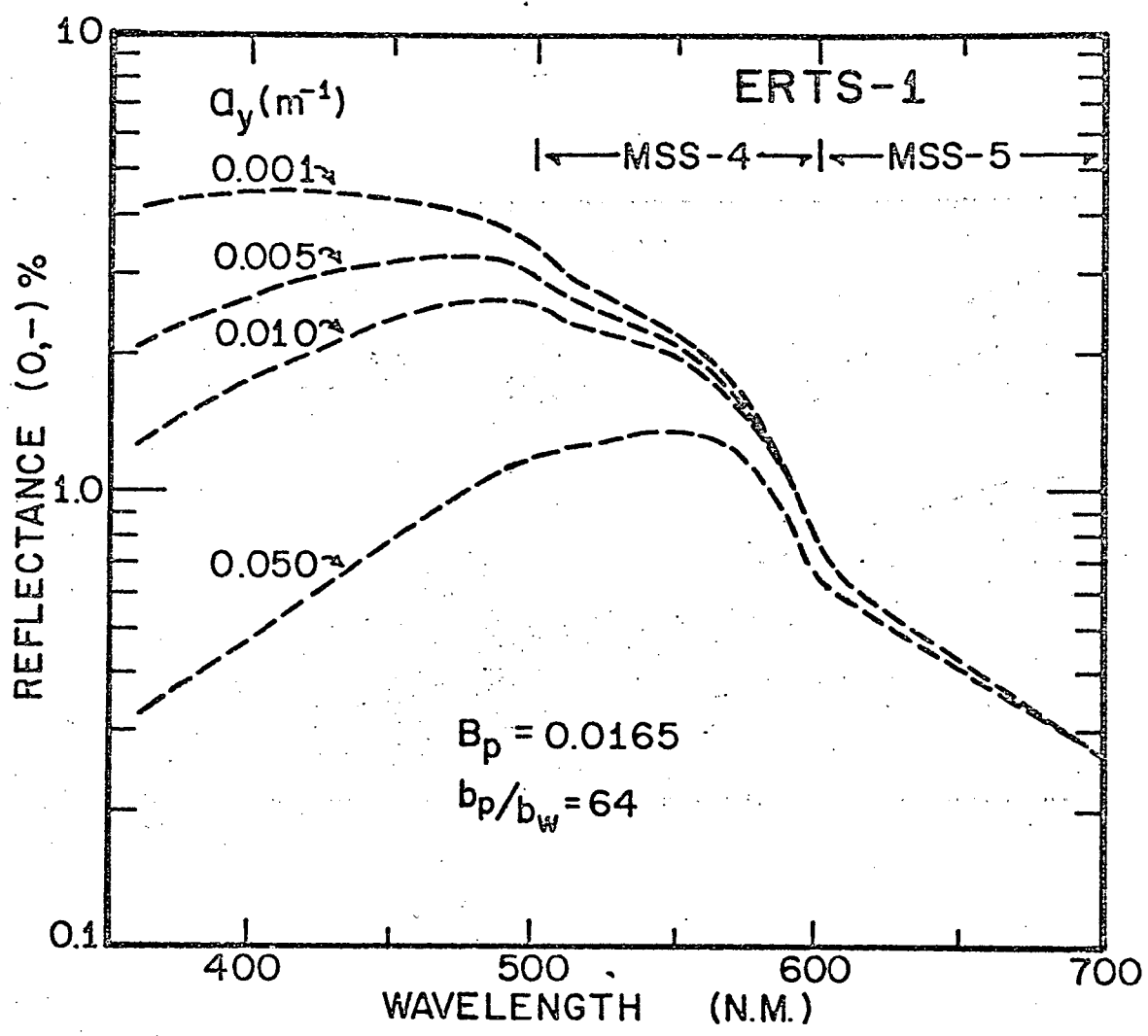


Figure 10. Computed reflectance spectra, in percent, at the sea surface. The ratio of the particle to water scattering coefficients (b_p/b_w) and the fraction of backscattered light are 128 and 0.0165 respectively. Values of the absorption coefficient due to yellow substance (a_y) are listed on the left hand side. Note the shift of the spectral peak to longer wavelengths with increasing a_y .